To be published in Optics Letters:

Title: Low-noise high-order Raman fiber laser pumped by random lasing

Authors: Bing Han,Yun-Jiang Rao,Han Wu,Jiazhen Yao,Hongjian Guan,Rui Ma,Zinan Wang

Accepted: 19 September 20

Posted 21 September 20

DOI: https://doi.org/10.1364/OL.405899

Low-noise high-order Raman fiber laser pumped by random lasing

BING HAN,[1] YUNJIANG RAO,[1,2,4] HAN WU[3,5], JIAZHEN YAO,[1] HONGJIAN GUAN,[1] RUI MA,[1] ZINAN WANG,[1]

[1] Key Lab of Optical Fiber Sensing & Communications, University of Electronic Science & Technology of China, Chengdu, Sichuan 611731, China
[2] Research Center for Optical Fiber Sensing, Zhejiang Laboratory, Hangzhou, Zhejiang 310000, China
[3] College of Electronics and Information Engineering, Sichuan University, Chengdu, Sichuan 610064, China
[4] yjrao@uestc.edu.cn
[5] hanwu@scu.edu.cn

Received XX Month XXXX; revised XX Month, XXXX; accepted XX Month XXXX; posted XX Month XXXX (Doc. ID XXXXX); published XX Month XXXX

Raman fiber lasers (RFLs) have been widely utilized in long-haul optical transmission systems as pump sources for distributed Raman amplification (DRA) to increase transmission distance and capacity. However, RFLs with relatively large temporal intensity fluctuations would deteriorate signal quality due to the transfer of relative intensity noise (RIN). In this letter, a low-noise high-order RFL common-cavity pumped by an ytterbium-doped random fiber laser (YRFL) is proposed and demonstrated, for the first time. Stable 4th-order random Raman lasing operating at 1365 nm is generated with 8.9 W of output power, without use of a multi-stage master oscillation power amplification (MOPA) system. Thanks to the YRFL common-cavity pumping where a wavelength division multiplexer (WDM)-assisted fiber-loop mirror is used to generate stable 1090 nm ytterbium-doped random lasing and cascaded random Raman lasing simultaneously, the RIN of the 1365 nm RFL is suppressed as low as -120 dB/Hz without any peak over 0-100 MHz span. Furthermore, the output power and lasing wavelength of this RFL can be flexibly tuned by adjusting LD pump power, high reflectivity fiber Bragg grating (HR FBG) center wavelength and single-mode fiber (SMF) length. Hence, such a low-noise high-order RFL paves a way for development of novel tunable RFLs with stable temporal output, leading to potential replacement of conventional RFLs for DRA in long-haul optical transmission systems to achieve better performances.

http://dx.doi.org/10.1364/OL.99.099999

In recent years, long-haul unrepeatered optical transmission technologies have been widely used in the fields of optical fiber communication and sensing, such as submarine communication, island connection and border security, et al [1-3]. To achieve hundreds of kilometers point-to-point transmission without any in-line repeaters, high-quality optical amplification is essential. Compared with lumped amplifiers, such as erbium-doped fiber amplifiers, DRA technology has become a key solution in long-haul unrepeatered systems with obvious advantages in terms of noise figure, nonlinear damage and gain bandwidth, which has successfully enhanced optical signal-to-noise ratio and avoid or mitigate nonlinear effects in optical transmission systems for many years [4]. Raman fiber lasers (RFLs) with good wavelength agility and power scalability are preferred as pump sources of DRA. Besides conventional cavity-based RFLs, random Raman fiber laser (RRFL) based on distributed Rayleigh scattering and Raman gain in long passive fiber with no resonant cavity has been reported as a novel RFL in 2010 [5]. Due to their intrinsic modeless property and structural simplicity [6], random fiber lasers have attracted extensive attentions in the past decade, and have been used as a new platform for designing a series of new laser sources with low noise [7, 8], high power/efficiency [9, 10], ultrawide wavelength tunability [11, 12], low spatial coherence [13, 14] and good temporal stability [15, 16], respectively. With these unique features, RRFLs have already found important applications as pump sources for DRA of optical communication and sensing systems [17, 18], mid-infrared fiber lasers [19, 20], speckle free imaging [21, 22] and laser frequency doubling [23], et al.

Compared to conventional RFLs with resonant cavities, RRFLs offer much better flexibility to realize laser emission in the wavelength region from 1.2 μm to 1.4 μm without needs of a series of fiber Bragg grating (FBG) pairs used to reflect the intermediate Stokes wavelengths [24]. In order to construct high-order RRFLs, ytterbium-doped fiber lasers (YFLs) formed by FBG pairs are normally acted as pump sources [25, 26]. However, the lasing output of this kind of high-order RRFLs suffers from relatively large temporal intensity fluctuations [25, 27], which is not favorable in DRA since the RIN transfer may seriously influence the signal quality in long-haul optical systems [25, 27-29].

Recently, high-order RRFLs pumped by filtered amplified spontaneous emission (ASE) generated by ytterbium-doped fiber (YDF) provide a new way to achieve stable temporal lasing output [26, 27]. Compared to YFL pumped RRFLs, high-order RRFLs based on filtered ASE pump have been verified to have superior performances including better temporal stability and higher spectrum purity [16, 27]. In these schemes, ASE sources can be tuned to desired wavelengths by employing a tunable bandpass filter. However, as the optical power of the filtered ASE pump is quite low (<100 mW), it has to be amplified by using a multi-stage MOPA system [16, 27]. Furthermore, special WDMs with high power-handling ability are required to inject the ASE pumping light into the RRFLs and extract all the intermediate Stokes light to the broadband reflector [27], leading to a significant increase in complexity and cost.

In this letter, we propose and demonstrate a novel low-noise high-order RFL that is common-cavity pumped by an YRFL, for the first time. Here, a WDM-assisted fiber-loop mirror is used to generate stable 1090 nm ytterbium-doped random lasing and cascaded random Raman lasing simultaneously. It is found that with the help of the modeless 1090 nm YRFL pump, such a 1365 nm high-order RFL has much better temporal stability compared to commercial 1365 nm cavity-based RFL pumped by YFL. Also, the output power of the 1365 nm random Raman lasing is measured as 8.9 W with no need of the MOPA system, which can meet the DRA requirement for long-haul transmission systems well. Therefore, it may be the best pump for DRA in long-haul optical transmission and sensing systems.

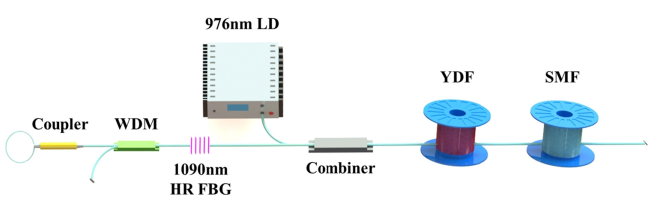

Fig. 1. Experimental setup of the high-order RFL pumped by the YRFL.

Figure 1 shows the schematic diagram of the high-order RFL pumped by the YRFL. When the laser diode (LD) pump injects into the YDF through the pump combiner, the 1090 nm YRFL occurs with the help of ytterbium-doped gain in the YDF, distributed Rayleigh scattering feedback in the SMF, and reflection of the 1090 nm HR FBG. Then the 1090 nm YRFL can further serve as direct pump to stimulate the random Raman lasing in the SMF. By adding a broadband mirror to the reflection port of the WDM, the pump combiner can also be utilized to extract the Stokes waves generated in the SMF and provide point feedback for the Stokes waves. In this way, a compact high-order RFL is constructed without using a series of specific FBGs. Furthermore, the output power and lasing wavelength of this RFL can be flexibly tuned by adjusting LD pump power, HR FBG center wavelength and SMF length. More importantly, by using the temporally stable YRFL pump, the RIN of the cascaded random Raman lasing can be suppressed to a very low level without any longitudinal mode beating due to the natural beauty of modeless random lasing.

A 976 nm multimode LD is used as primary pump source. The LD pump is injected into a 5 m long 10/130 μm double-cladding YDF (Nufern LMA-YDF-10/130-VIII) via a (2+1) × 1 pump combiner. A 4.15 km long SMF is used to provide random distributed Rayleigh feedback and Raman gain. The peak reflectivity of the 1090 nm HR FBG is 99.5%. As a key design, the output of the 1090 nm HR FBG is connected to a 1080 nm/1200 nm WDM (pass port: 1070-1090 nm, reflection port: 1150-1400nm). Since the YRFL is the direct pump for random Raman lasing, in order to generate stable YRFL assisted by 1090 nm FBG, the 1080 nm port of WDM is angle-cleaved to avoid the reflection of other wavelengths in YDF gain band which will result in the generation of broadband unstable ytterbium doped self-random-lasing with many random spikes [30]. The 1200 nm port of the WDM is spliced to a 50:50 optical coupler with output ports fused together to form a fiber-loop mirror to provide sufficient broadband point feedback for intermediate Raman Stokes wavelengths. As the forward-pumped short cavity RFL with moderate reflectivity point reflector can generate high efficiency random Raman lasing [31], the YRFL pump, the WDM-assisted fiber-loop mirror, the distributed Rayleigh feedback and Raman gain in the SMF, are all combined to form such a forward-pumped structure for generating cascaded random Raman lasing in this work. The end of the SMF is angle-cleaved to avoid the unwanted backward reflection, and also serves as the output port of the laser. The injected LD pump power is measured after the pump combiner, while the laser output is measured at far end of the SMF. To record spectral and time domain properties of the YRFL and the high-order RFL, a 1:99 optical coupler is connected to the end of the SMF and the 1% port is used as the monitoring port.

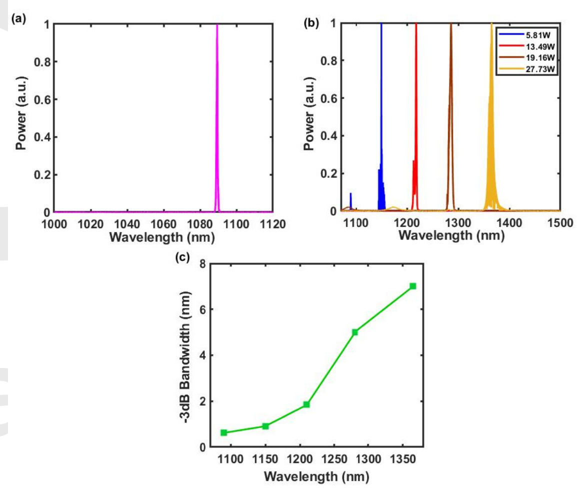

Fig. 2. (a) Normalized spectrum of the 1090 nm YRFL pump. (b) Normalized spectra of the 1st to 4th-order random Raman lasing. (c) -3 dB bandwidths of the 1090 nm YRFL pump and the 1st to 4th-order random Raman lasing.

The spectra in Fig. 2 are measured by an optical spectrum analyzer (OSA, Ando AQ6317B) with 0.02 nm resolution. Figure 2(a) shows the normalized spectrum in linear scale of 0.8 W 1090 nm YRFL at 2.93 W LD pump power. It can be seen that by employing the WDM, the output spectrum of the YRFL exhibits stable single-peak behavior and ensures generation of temporal stable high-order RFL. Figure 2(b) shows the normalized spectra of the 1st to 4th-order random Raman lasing measured as LD pump power being 5.81 W, 13.49 W, 19.16 W and 27.73 W, respectively. With increase in the LD pump power, the YRFL stimulates random Raman lasing in the SMF and the cascaded operation for random Raman lasing simultaneously. The center wavelengths of the 1st to 4th-order random Raman lasing are located at 1150 nm, 1210 nm, 1280 nm and 1365 nm, respectively. Figure 2(c) depicts -3 dB bandwidths of the 1090 nm YRFL and each order random Raman lasing measured with the same LD pump power to that in Fig. 2(a) and (b). The -3 dB bandwidth of the 1090 nm YRFL and the 1150nm, 1210 nm, 1280 nm and 1365 nm random Raman lasing are 0.62 nm, 0.91 nm, 1.84 nm, 4.95 nm and 6.98 nm, respectively.

The output power evolution of the 1090 nm YRFL and the 1st to 4th-order random Raman lasing versus the LD pump power is shown in Fig. 3. The 1090 nm YRFL pump output power increases linearly with the LD pump power in the initial stage. The threshold power of the LD pump for the 1150 nm, 1210 nm, 1280 nm, and 1365 nm random Raman lasing generation is measured as 3.63 W, 6.63 W, 13.75 W and 19.92 W, respectively. The random Raman lasing power grows nonlinearly after reaching the threshold, and the maximum output power increases with the Raman Stokes order. When the 1st-order random Raman lasing occurs, the 1090 nm YRFL pump power starts to deplete in the SMF. Then, the output power of the lower order random Raman lasing decreases with the similar behavior when the higher order random Raman lasing occurs. The highest output power of the 1365 nm random Raman lasing is 8.9 W at 27.73 W LD pump power, and the optical conversion efficiency from the 976 nm LD to the 1365 nm high-order RFL is ~32%. The maximum output power and conversion efficiency can be further improved by optimizing the length of the SMF and the reflectivity of the fiber-loop mirror [5].

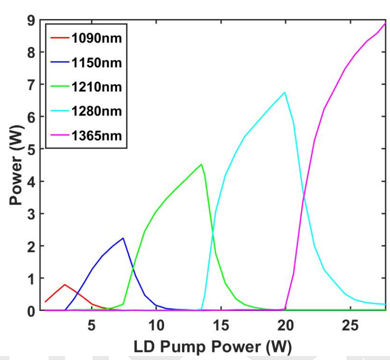

Fig. 3. Output power of the 1090 nm YRFL pump and 1st to 4th-order random Raman lasing versus LD pump power.

In our case, the 1090 nm YRFL is the direct pump for random Raman lasing generation. Since pump temporal dynamics will influence temporal stability of random Raman lasing, we measured the temporal performances of both the 1090 nm YRFL pump and the 1365 nm random Raman lasing. The temporal characteristics of the lasing output are measured by a photodetector (PD) with 400 MHz bandwidth and an oscilloscope with 1 GHz bandwidth. Figure 4(a) and blue line in Fig. 5(a) show the normalized time domain traces of the 1090 nm YRFL pump at 2.93 W LD pump power and the 1365 nm random Raman lasing at 27.73 W LD pump power in 50 ms span. It can be seen that both the 1090 nm YRFL pump and the 1365 nm random Raman lasing exhibit quasi-continuous wave output behavior with good temporal stability. The standard deviations versus mean values of the stable 1090 nm YRFL pump and the 1365 nm random Raman lasing are 3.6% and 4.41%, respectively. Meanwhile, the RIN of the 1090 nm YRFL pump at 2.93 W LD pump power and the 1365 nm random Raman lasing at 27.73 W LD pump power are also measured by employing an electrical spectrum analyzer. Since RIN transfer in Raman amplification mainly exists within tens of megahertz bandwidth, the RIN spectrum in this work is measured in a span of 0-100 MHz [32]. The results are shown in Fig. 4(b) and the blue line in Fig. 5(b). For the RIN spectrum measurements, the resolution bandwidth is set as 1 kHz. One can see that the radio frequency (RF) spectrum of the 1090 nm YRFL pump has the modeless feature. This means that the temporal intensity of the YRFL pump shows stochastic fluctuations without regular high contrast pulses caused by stationary mode beating in conventional cavity-based YFL [33]. Pumping by the modeless 1090 nm YRFL, the 1365 nm RRFL also inherits modeless spectrum property in frequency domain (see in the blue line of Fig. 5(b)). Moreover, the blue line in the insert of Fig. 5(b) shows that there is no longitudinal mode beating corresponding to 4.15 km SMF length, verifying that there is no resonance frequency in the YRFL pumped high-order RRFL proposed. The measured RIN value of the 1090 nm YRFL pump and the 1365 nm random Raman lasing are both ~-120 dB/Hz. Although the operation principle of such a low-noise RFL has been verified by experiment, further theoretical work still needs to be done to analyze the RIN of the YRFL and RRFL, and the RIN transfer properties from the YRFL to the cascaded RRFL [29, 34].

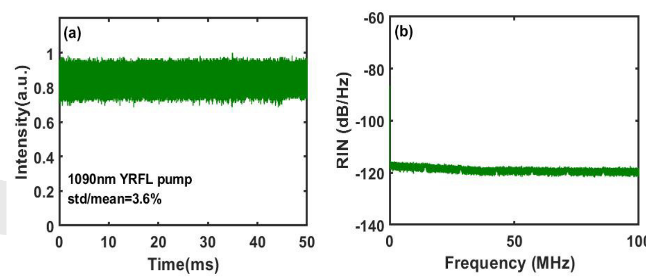

Fig. 4. (a) Time domain trace of the 1090 nm YRFL pump. (b) RIN of the 1090 nm YRFL pump.

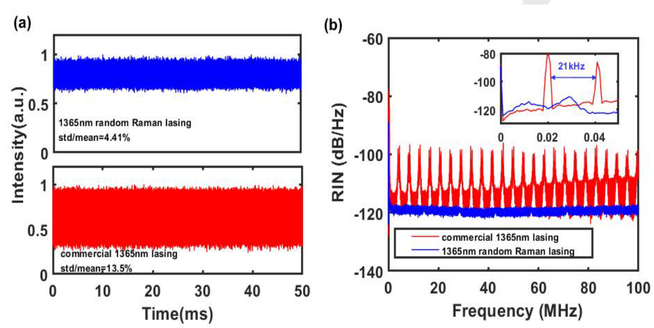

Fig. 5. (a) Time domain traces of the 1365 nm random Raman lasing and the commercial 1365 nm pump. (b) RIN of the 1365 nm random Raman lasing and commercial 1365 nm pump. Insert: Enlarged view in

0-0.05MHz span. Blue line: 1365 nm random Raman lasing; Red line: commercial 1365 nm lasing.

As comparison, we also measured the temporal stability of a commercial 1365 nm RFL (Keopsys KPS-CUS-BT-RFL-1366) with 5 W maximum output power. The commercial RFL is formed in a conventional cavity-based configuration pumped by YFL. As shown in the red line of Fig. 5(a), the intensity fluctuation in the commercial RFL is severe, as the measured standard deviation versus mean value is 13.5%. It can be seen from the red line of Fig. 5(b), there are periodical peaks with the RIN of -100 dB/Hz in RF spectrum of the commercial RFL, which is ~20 dB higher than the RIN of the RFL demonstrated in this work. These peaks corresponding to the cavity length of the YFL pump, confirming that the power fluctuation of the pump laser (YFL) is transferred directly to the Raman outputs through cascade Raman scattering process [23, 34]. The temporal dynamics of conventional YFLs commonly suffer from self-pulsing, self-mode locking and turbulence-like pulsing, resulting in relatively large intensity fluctuations [35, 36], which will deteriorate temporal stability of cascaded RFLs considerably. The red line in the insert of Fig. 5(b) shows the existence of longitudinal mode with ~21 kHz spacing, corresponding to the cavity length of the commercial RFL. We should note that for YFL-pumped RRFL, RIN transfer from YFL to high-order random Raman lasing still exists, and would cause poor temporal stability of high-order RRFL [23, 25, 27, 34].

In conclusion, a temporally stable high-order RFL with YRFL pumping is reported, for the first time. By employing a common-cavity with feedback from a WDM-assisted fiber-loop mirror, the generated 1090 nm ytterbium-doped random fiber lasing acts as the RFL pump. The 4th-order random Raman lasing at 1365 nm has been experimentally obtained with output power of 8.9 W. Moreover, with the modeless YRFL pump, the proposed high-order RFL shows peak-less feature with much better temporal stability where its RIN is measured as low as -120 dB/Hz. In contrast, the RIN spectrum of a commercial 1365 nm RFL pumped by a cavity-based YFL shows periodical peaks with RIN that is 20 dB higher than that of the 1365 nm RFL demonstrated in this work. Thus, such a type of novel low-noise high-order RFL, offering advantages of high-power, low-RIN, good-stability, excellent cost-effectivity, flexible tunability, et al, may become the best candidate as an ideal pump source for DRA applications in long-haul optical fiber communication and sensing systems.

Funding. National Natural Science Foundation of China (61635005, 41527805), and the 111 project (B14039).

Disclosures. The authors declare no conflicts of interest.

References

1. H. Bissessur, C. Bastide, S. Dubost, S. Etienne, F. Hedaraly, and M. Duval, 45th European Conference on Optical Communication, (IET 2019), 0801.
2. P. Rosa, G. Rizzelli, X. Pang, O. Ozolins, A. Udalcovs, M. Tan, M. Jaworski, M. Marciniak, S. Sergeyev, R. Schatz, G. Jacobsen, S. Popov and J. D. Ania-Castañón, Appl. Sci. **10**, 1433 (2020).
3. H. J. Wu, Z. N. Wang, F. Peng, Z. P. Peng, X. Y. Li, Y. Wu, Y. J. Rao, in International Conference on Optical Fiber Sensors, (OSA 2014), 915790.
4. J. Bromage, J. Lightwave Technol. **22**, 79-93 (2004).
5. S. K. Turitsyn, S. A. Babin, A. E. El-Taher, P. Harper, D. V. Churkin, S. I. Kablukov, J. D. Ania-Castanon, V. Karalekas, and E. V. Podivilov, Nat. Photon. **4**, 231-235 (2010).
6. D. V. Churkin, S. Sugavanam, I. D. Vatnik, Z. N. Wang, E. V. Podivilov, S. A. Babin, Y. J. Rao, and S. K. Turitsyn, Advances in Optics and Photonics, **7**, 516-569 (2015).
7. B. Saxena, X. Bao, and L. Chen, Opt. Lett. **39**, 1038-1041 (2014).
8. Z. Zhou, P. Lu, L. Zhang, S. Mihailov, L. Chen, and X. Bao, Opt. Lett. **44**, 4195-4198 (2019).
9. I. D. Vatnik, D. V. Churkin, E. V. Podivilov, and S. A. Babin, Laser Phys. Lett. **11**, 075101 (2014).
10. Z. Wang, H. Wu, M. Fan, L. Zhang, Y. Rao, W. Zhang, and X. Jia, IEEE J. Sel. Top. Quantum Electron. **21**, 0900506 (2015).
11. L. Zhang, H. W. Jiang, X. Z. Yang, W. W. Pan, and Y. Feng, Opt. Lett. **41**, 215-218 (2016).
12. V. Balaswamy, S. Aparanji, S. Arun, S. Ramachandran, and V. R. Supradeepa, Opt. Lett. **44**, 279-282 (2019).
13. R. Ma, Z. Wang, H. H. Zhang, W. L. Zhang, and Y. J. Rao, Opt. Lett. **45**, 3816-3819 (2020).
14. R. Ma, J. Q. Li, J. Y. Guo, H. Wu, H. H. Zhang, B. Hu, Y. J. Rao, and W. L. Zhang, Opt. Express, **27**, 8738-8744 (2019).
15. J. X. Song, H. S. Wu, J. Ye, J. M. Xu, H. W. Zhang, and P. Zhou, Photonic Sensors, **9**, 43-48 (2019).
16. J. Xu, J. Ye, H. Xiao, J. Leng, W. Liu, and P. Zhou, High Power Laser Sci. Eng. **6**, e46 (2018).
17. M. Tan, P. Rosa, S. T. Le, Md. A. Iqbal, I. D. Phillips, and P. Harper, Opt. Express, **24**, 2215-2221 (2016).
18. X. Jia, Y. Rao, C. Yuan, J. Li, X. Yan, Z. Wang, W. Zhang, H. Wu, Y. Zhu, and F. Peng, Opt. Express, **21**, 24611-24619 (2013).
19. H. Zhang, P. Zhou, X. Wang, X. Du, H. Xiao, and X. Xu, Opt. Express, **23**, 17138–17144 (2015).
20. H. S. Wu, P. Wang, J. X. Song, J. Ye, J. M. Xu, X. Li, and P. Zhou, Opt. Express, **26**, 6446-6455 (2018).
21. B. Redding, M. A. Choma, and H. Cao, Nat. Photon. **6**, 355–359 (2012).
22. R. Ma, Y. J. Rao, W. L. Zhang, and B. Hu, IEEE J. Sel. Top. Quantum Electron. **25**, 0900106 (2019).
23. E. I. Dontsova, S. I. Kablukov, I. D. Vatnik, and S. A. Babin, Opt. Lett. **41**, 1439-1442 (2016).
24. V. R. Supradeepa, Y. Feng, and J. W. Nicholson, J. Opt. **19**, 023001 (2017).
25. Y. Fu, R. C. Zhu, B. Han, H. Wu, Y. J. Rao, C. Y. Lu, and Z. N. Wang, J. Lightwave Technol. **37**, 4680-4686 (2019).
26. V. Balaswamy, S. Ramachandran, and V. R. Supradeepa, Opt. Express, **27**, 9725-9732 (2019).
27. J. Y. Dong, L. Zhang, H. W. Jiang, X. Z. Yang, W. W. Pan, S. Z. Cui, and Y. Feng, Opt. Express, **26**, 5275-5280 (2018).
28. P. Rosa, G. Rizzelli, M. Tan, et al. Opt. Express, **23**, 28634-28639 (2015).
29. S. Rota-Rodrigo, G. Rizzelli, D. Leandro, J. Nuño, M. Lopez-Amo, G. Santarelli, and J. Ania-Castañón, Opt. Express, **28**, 28234-28242 (2020).
30. H. Wu, Z. Wang, Q. He, W. Sun, and Y. Rao, Laser Phys. Lett. **14**, 065101 (2017).
31. H. Wu, Z. Wang, M. Fan, L. Zhang, W. Zhang, and Y. Rao, Opt. Express, **23**, 1421-1427 (2015).
32. W. S. Pelouch, J. Lightwave Technol. **34**, 6-19 (2016).
33. H. Wu, B. Han, Z. Wang, G. Genty, G. Feng, and H. Liang, Opt. Express, **28**, 9957-9964 (2020).
34. J. Nuno, M. Alcon-Camas, and J. D. Ania-Castanon, Opt. Express, **20**, 27376-27381 (2012).
35. B. N. Upadhyaya, A. Kuruvilla, U. Chakravarty, M. R. Shenoy, K. Thyagarajan, and S. M. Oak, Appl. Opt. **49**, 2316-2325 (2010).
36. W. Liu, P. F. Ma, P. Zhou, Z. F. Jiang, International Symposium on Optoelectronic Technology and Application, (2018), 1084407.

References

1. H. Bissessur, C. Bastide, S. Dubost, S. Etienne, F. Hedaraly, and M. Duval, "Record single fibre unrepeatered transmission of 2 × 500 Gb/s over 405.7 km," 45th European Conference on Optical Communication, (IET 2019), 0801.
2. P. Rosa, G. Rizzelli, X. Pang, O. Ozolins, A. Udalcovs, M. Tan, M. Jaworski, M. Marciniak, S. Sergeyev, R. Schatz, G. Jacobsen, S. Popov and J. D. Ania-Castañón, "Unrepeatered 240-km 64-QAM Transmission Using Distributed Raman Amplification over SMF Fiber," Appl. Sci. 10(4), 1433 (2020).
3. H. J. Wu, Z. N. Wang, F. Peng, Z. P. Peng, X. Y. Li, Y. Wu, Y. J. Rao, "Field test of a fully distributed fiber optic intrusion detection system for long-distance security monitoring of national borderline," in International Conference on Optical Fiber Sensors, (OSA 2014), 915790.
4. J. Bromage, "Raman Amplification for Fiber Communications Systems," J. Lightwave Technol. 22(1), 79-93 (2004).
5. S. K. Turitsyn, S. A. Babin, A. E. El-Taher, P. Harper, D. V. Churkin, S. I. Kablukov, J. D. Ania-Castanon, V. Karalekas, and E. V. Podivilov, "Random distributed feedback fibre laser," Nat. Photon. 4(4), 231-235 (2010).
6. D. V. Churkin, S. Sugavanam, I. D. Vatnik, Z. N. Wang, E. V. Podivilov, S. A. Babin, Y. J. Rao, and S. K. Turitsyn, "Recent advances in fundamentals and applications of random fiber lasers," Advances in Optics and Photonics, 7(3), 516-569 (2015).
7. B. Saxena, X. Bao, and L. Chen, "Suppression of thermal frequency noise in erbium-doped fiber random lasers," Opt. Lett. 39(4), 1038-1041 (2014).
8. Z. Zhou, P. Lu, L. Zhang, S. Mihailov, L. Chen, and X. Bao, "Thermal and acoustic noise insensitive Brillouin random fiber laser based on polarization-maintaining random fiber grating," Opt. Lett. 44(17), 4195-4198 (2019).
9. I. D. Vatnik, D. V. Churkin, E. V. Podivilov, and S. A. Babin, "High-efficiency generation in a short random fiber laser," Laser Phys. Lett. 11(7), 075101 (2014).
10. Z. Wang, H. Wu, M. Fan, L. Zhang, Y. Rao, W. Zhang, and X. Jia, "High power random fiber laser with short cavity length: theoretical and experimental investigations," IEEE J. Sel. Top. Quantum Electron. 21(1), 0900506 (2015).
11. L. Zhang, H. W. Jiang, X. Z. Yang, W. W. Pan, and Y. Feng, "Ultra-wide wavelength tuning of a cascaded Raman random fiber laser," Opt. Lett. 41(2), 215-218 (2016).
12. V. Balaswamy, S. Aparanji, S. Arun, S. Ramachandran, and V. R. Supradeepa, "High-power, widely wavelength tunable, grating free Raman fiber laser based on filtered feedback," Opt. Lett. 44(2), 279-282 (2019).
13. R. Ma, Z. Wang, H. H. Zhang, W. L. Zhang, and Y. J. Rao, "Imaging through opacity using a near-infrared low-spatial-coherence fiber light source," Opt. Lett. 45(13), 3816-3819 (2020).
14. R. Ma, J. Q. Li, J. Y. Guo, H. Wu, H. H. Zhang, B. Hu, Y. J. Rao, and W. L. Zhang, "High-power low spatial coherence random fiber laser," Opt. Express, 27(6), 8738-8744 (2019).
15. J. X. Song, H. S. Wu, J. Ye, J. M. Xu, H. W. Zhang, and P. Zhou, "High Power Linearly Polarized Raman Fiber Laser With Stable Temporal Output," Photonic Sensors, 9(1), 43-48 (2019).
16. J. Xu, J. Ye, H. Xiao, J. Leng, W. Liu, and P. Zhou, "In-band pumping avenue based high power superfluorescent fiber source with record power and near-diffraction-limited beam quality," High Power Laser Sci. Eng. 6, e46 (2018).
17. M. Tan, P. Rosa, S. T. Le, Md. A. Iqbal, I. D. Phillips, and P. Harper, "Transmission performance improvement using random DFB laser based Raman amplification and bidirectional second-order pumping," Opt. Express, 24(3), 2215-2221 (2016).
18. X. Jia, Y. Rao, C. Yuan, J. Li, X. Yan, Z. Wang, W. Zhang, H. Wu, Y. Zhu, and F. Peng, "Hybrid distributed Raman amplification combining random fiber laser based 2nd-order and low-noise LD based 1st-order pumping," Opt. Express, 21(21), 24611-24619 (2013).
19. H. Zhang, P. Zhou, X. Wang, X. Du, H. Xiao, and X. Xu, "Hundred-watt-level high power random distributed feedback Raman fiber laser at 1150 nm and its application in mid-infrared laser generation," Opt. Express 23(13), 17138–17144 (2015).
20. H. S. Wu, P. Wang, J. X. Song, J. Ye, J. M. Xu, X. Li, and P. Zhou, "High power tunable mid-infrared optical parametric oscillator enabled by random fiber laser," Opt. Express, 26(5), 6446-6455 (2018).
21. B. Redding, M. A. Choma, and H. Cao, "Speckle-free laser imaging using random laser illumination," Nat. Photon. 6(6), 355–359 (2012).
22. R. Ma, Y. J. Rao, W. L. Zhang, and B. Hu, "Multimode random fiber laser for speckle-free imaging," IEEE J. Sel. Top. Quantum Electron. 25(1), 0900106 (2019).
23. E. I. Dontsova, S. I. Kablukov, I. D. Vatnik, and S. A. Babin, "Frequency doubling of Raman fiber lasers with random distributed feedback," Opt. Lett. 41(7), 1439-1442 (2016).
24. V. R. Supradeepa, Y. Feng, and J. W. Nicholson, "Raman fiber lasers," J. Opt. 19(2017), 023001 (2017).
25. Y. Fu, R. C. Zhu, B. Han, H. Wu, Y. J. Rao, C. Y. Lu, and Z. N. Wang, "175-km Repeaterless BOTDA With Hybrid High-Order Random Fiber Laser Amplification," J. Lightwave Technol. 37(18), 4680-4686 (2019).
26. V. Balaswamy, S. Ramachandran, and V. R. Supradeepa, "High-power, cascaded random Raman fiber laser with near complete conversion over wide wavelength and power tuning," Opt. Express, 27(7), 9725-9732 (2019).
27. J. Y. Dong, L. Zhang, H. W. Jiang, X. Z. Yang, W. W. Pan, S. Z. Cui, and Y. Feng, "High order cascaded Raman random fiber laser with high spectral purity," Opt. Express, 26(5), 5275-5280 (2018).
28. P. Rosa, G. Rizzelli, M. Tan, et al. "Characterisation of random DFB Raman laser amplifier for WDM transmission," Opt. Express, 23(22), 28634-28639 (2015).
29. S. Rota-Rodrigo, G. Rizzelli, D. Leandro, J. Nuño, M. Lopez-Amo, G. Santarelli, and J. Ania-Castañón, "Anomalous relative intensity noise transfer in ultralong random fiber lasers," Opt. Express, 28(19), 28234-28242 (2020).
30. H. Wu, Z. Wang, Q. He, W. Sun, and Y. Rao, "Common-cavity ytterbium/Raman random distributed feedback fiber laser," Laser Phys. Lett. 14(6), 065101 (2017).
31. H. Wu, Z. Wang, M. Fan, L. Zhang, W. Zhang, and Y. Rao, "Role of the mirror's reflectivity in forward-pumped random fiber laser," Opt. Express, 23(2), 1421-1427 (2015).
32. W. S. Pelouch, "Raman amplification: an enabling technology for long-haul coherent transmission systems," J. Lightwave Technol. 34(1), 6-19 (2016).
33. H. Wu, B. Han, Z. Wang, G. Genty, G. Feng, and H. Liang, "Temporal ghost imaging with random fiber lasers," Opt. Express, 28(7), 9957-9964 (2020).
34. J. Nuno, M. Alcon-Camas, and J. D. Ania-Castanon, "RIN transfer in random distributed feedback fiber lasers," Opt. Express, 20(24), 27376-27381 (2012).
35. B. N. Upadhyaya, A. Kuruvilla, U. Chakravarty, M. R. Shenoy, K. Thyagarajan, and S. M. Oak, "Effect of laser linewidth and fiber length

on self-pulsing dynamics and output stabilization of single-mode Yb-doped double-clad fiber laser," Appl. Opt. 49(12), 2316-2325 (2010).
36. W. Liu, P. F. Ma, P. Zhou, Z. F. Jiang, "Unified theory of the temporal spectral dynamics in ytterbium-doped fiber lasers," International Symposium on Optoelectronic Technology and Application, (2018), 1084407.